Three-dimensional polarimetric computational integral imaging

Xiao Xiao,[1] Bahram Javidi,[1,*] Genaro Saavedra,[2] Michael Eismann,[3] and Manuel Martinez-Corral[2]

[1]*Electrical and Computer Engineering Department, University of Connecticut, 371 Fairfield Rd, Unit 2157, Storrs, CT 06269-2157, USA*
[2]*Department of Optics, University of Valencia, c/ Dr. Moliner 50. E-46100 Burjassot, Spain*
[3]*Sensors Directorate, Air Force Research Laboratory, Wright-Patterson AFB, Ohio, USA*
[*]*bahram.javidi@uconn.edu*

Abstract: In this paper, we propose a novel 3D polarimetric computational integral imaging system by using polarization diversity of objects under natural illumination conditions. In the system, the measured Stokes polarization parameters are utilized to generate degree of polarization images of a 3D scene. Based on degree of polarization images and original 2D images, we utilize a modified computational reconstruction method to perform 3D polarimetric image reconstruction. The system may be used to detect or classify objects with distinct polarization signatures in 3D space. Experimental results also show the proposed system may mitigate the effect of occlusion in 3D reconstruction.

OCIS codes: (100.6890) Three-dimensional image processing; (120.5410) Polarimetry; (110.6880) Three-dimensional image acquisition; (150.6910) Three-dimensional sensing.

References and links

1. H. S. Chen and C. Rao, "Polarization of light on reflection by some natural surfaces," J. Phys. D **1**(9), 1191–1200 (1968).
2. T. H. Waterman, "Polarization sensitivity," Handbook of sensory physiology **7,** 281–469 (1981).
3. L. B. Wolff, "Polarization-based material classification from specular reflection," IEEE Trans. Pattern Anal. Mach. Intell. **12**(11), 1059–1071 (1990).
4. L. B. Wolff, "Polarization vision: a new sensory approach to image understanding," Image Vision Comput. **15**, 81–93 (1997).
5. S. Daly, "Polarimetric imaging," Rochester Institute of Technology, 2002, (technical report).
6. M. I. Mishchenko, Y. S. Yatskiv, V. K. Rosenbush, and G. Videen, *Polarimetric Detection, Characterization, and Remote Sensing* (Springer, 2011).
7. G. Lippmann, "La photographie integrale," CR Acad. Sci. **146**, 446–451 (1908).
8. H. E. Ives, "Optical properties of a Lippman lenticulated sheet," J. Opt. Soc. Am. A **21**(3), 171–176 (1931).
9. C. B. Burckhardt, "Optimum parameters and resolution limitation of integral photography," J. Opt. Soc. Am. **58**(1), 71–74 (1968).
10. T. Okoshi, "Three-dimensional displays," Proc. IEEE **68**(5), 548–564 (1980).
11. H. Arimoto and B. Javidi, "Integral three-dimensional imaging with digital reconstruction," Opt. Lett. **26**(3), 157–159 (2001).
12. S. H. Hong, J. S. Jang, and B. Javidi, "Three-dimensional volumetric object reconstruction using computational integral imaging," Opt. Express **12**(3), 483–491 (2004).
13. M. Martinez-Corral, B. Javidi, R. Martínez-Cuenca, and G. Saavedra, "Formation of real, orthoscopic integral images by smart pixel mapping," Opt. Express **13**(23), 9175–9180 (2005).
14. F. Okano, J. Arai, K. Mitani, and M. Okui, "Real-time integral imaging based on extremely high resolution video system," Proc. IEEE **94**(3), 490–501 (2006).
15. A. Stern and B. Javidi, "3D image sensing, visualization, and processing using integral imaging," Proc. IEEE **94**, 591–608 (2006).
16. M. DaneshPanah and B. Javidi, "Profilometry and optical slicing by passive three-dimensional imaging," Opt. Lett. **34**(7), 1105–1107 (2009).
17. R. Martinez-Cuenca, G. Saavedra, M. Martinez-Corral, and B. Javidi, "Progress in 3-D multiperspective display by integral imaging," Proc. IEEE **97**(6), 1067–1077 (2009).
18. B. Javidi, F. Okano, and J. Y. Son, *Three-dimensional Imaging, Visualization, and Display* (Springer, 2009).
19. M. Pollefeys, R. Koch, M. Vergauwen, A. A. Deknuydt, and L. J. Van Gool, "Three-dimensional scene reconstruction from images," Proc. SPIE **3958**, 215–226 (2000).

20. L. Guan, J. S. Franco, E. Boyer, and M. Pollefeys, "Probabilistic 3D occupancy flow with latent silhouette cues," IEEE Conference on Computer Vision and Pattern Recognition (CVPR) 1379–1386 (2010).
21. O. Matoba and B. Javidi, "Three-dimensional polarimetric integral imaging," Opt. Lett. **29**(20), 2375–2377 (2004).
22. B. Javidi, S. H. Hong, and O. Matoba, "Multidimensional optical sensor and imaging system," Appl. Opt. **45**(13), 2986–2994 (2006).
23. F. A. Sadjadi, "Passive three-dimensional imaging using polarimetric diversity," Opt. Lett. **32**(3), 229–231 (2007).
24. P. Miché, A. Bensrhair, and D. Lebrun, "Passive 3-D shape recovery of unknown objects using cooperative polarimetric and radiometric stereo vision processes," Opt. Eng. **44**(2), 027005 (2005).
25. K. E. Torrance and E. M. Sparrow, "Theory for off-specular reflection from roughened surfaces," J. Opt. Soc. Am. A **57**(9), 1105–1112 (1967).
26. R. B. Reid, M. E. Oxley, M. T. Eismann, and M. E. Goda, "Quantifying surface normal estimation," Proc. SPIE **6240**, 624001, 624001-11 (2006).
27. E. Collett, *Polarized Light: Fundamentals and Applications* (Marcel Dekker, 1993).
28. E. Wolf, *Introduction to the Theory of Coherence and Polarization of Light* (Cambridge University Press, 2007).
29. B. Schaefer, E. Collett, R. Smyth, D. Barrett, and B. Fraher, "Measuring the stokes polarization parameters," Am. J. Phys. **75**(2), 163–168 (2007).
30. J. S. Jang and B. Javidi, "Three-dimensional synthetic aperture integral imaging," Opt. Lett. **27**(13), 1144–1146 (2002).

1. Introduction

Light polarization can provide an important visual extension and enhance the capabilities of image understanding compared to only intensity imagery. Polarimetric imaging measures the polarization states of light coming from all points in a scene to obtain relevant information about the surfaces of materials. Therefore, these polarization properties can help to classify materials or identify objects of interest in industries, remote sensing and military applications [1–6].

3D imaging technologies [7–20] have been extensively studied during the past several decades with the goal of obtaining 3D information from 2D imagery. Among these technologies, integral imaging [7–18] has been the subject of a significant research effort for its unique properties. It obtains 3D scene information by recording traditional 2D images from multiple perspectives. Multiple 2D images (known as elemental images) can be captured by using a single image sensor with a lenslet array or an array of image sensors. Then, with the known sensor positions, a 3D scene can be computationally reconstructed in volume, represented by plane-by-plane images, based on the back-projection technique [12].

Recently, passive 3D polarimetric imaging has been researched [21–24]. In [21,22], a 3D polarimetric integral imaging system was first proposed. This system was implemented by illuminating 3D objects with a linearly polarized light and using a rotating linear polarizer-analyzer to determine Jones vector of elliptically polarized reflected light. Methods have also been developed to extract 3D shape information from polarimetric imagery through the relationship between the surface normal and the angle or degree of reflected or emitted polarization [23,24]. While these techniques offer the potential to extract 3D information from single polarimetric images, there are limitations to the estimation process due to the complexity of the relationship between the polarimetric measurements and the surface normal; this includes the dependence on unknown parameters such as the material optical constants and surface roughness [25,26]. Such methods also do not exhibit the ability to image through occlusions supported by integral imaging.

In this paper, we propose a novel 3D polarimetric integral imaging system by using degree of polarization (DoP) images under natural illumination conditions. Stokes polarization parameters are measured to generate DoP images. Then by using DoP images and the original elemental images, we present a modified computational reconstruction method to perform 3D polarimetric reconstruction. This proposed 3D polarimetric integral imaging may distinguish objects with specular-reflection surfaces (metal, glass) and objects with diffuse-reflection surfaces (soil, grass). Experimental results show that the proposed system may mitigate occlusion when surfaces of the occlusion and the occluded objects have different polarization properties.

#165278 - $15.00 USD Received 23 Mar 2012; revised 25 May 2012; accepted 28 May 2012; published 25 Jun 2012

2. Degree of polarization images

Here we briefly introduce the measurement of Stokes polarization parameters and the calculation method of degree of polarization. In our work, we use 2D images, namely DoP images, to illustrate DoP information of a scene,

Polarization of light is characterized by the relationship between the temporal average of magnitude and phase of two independent orthogonal electric field components. Stokes polarization parameters are widely used to describe the polarization state of light [27,28]. The four Stokes polarization parameters for a quasi-monochromatic light are defined by

$$\mathbf{S} = \begin{pmatrix} S_0 \\ S_1 \\ S_2 \\ S_3 \end{pmatrix} = \begin{pmatrix} \left\langle E_x^2 + E_y^2 \right\rangle \\ \left\langle E_x^2 - E_y^2 \right\rangle \\ 2\left\langle E_x E_y \cos\delta \right\rangle \\ 2\left\langle E_x E_y \sin\delta \right\rangle \end{pmatrix} \tag{1}$$

where S_i is the Stokes parameter of interest (i = [0, 1, 2, 3]), E_x and E_y are the maximum amplitudes of the x and y components of the electric field, and δ is the phase difference between the orthogonal components of the electric field. Angular brackets in (1) denote a temporal average. Note that a general beam is composed of natural (unpolarized) and completely polarized light. The parameter S_0 represents the total irradiance of the electric field while S_1 describes the relationship between the irradiance of linearly horizontally polarized and linearly vertically polarized components in the light beam. Similarly, S_2 describes the relationship between the linear + 45þ polarized component and the linear −45þ polarized component, and S_3 characterizes the part of circular polarization in the field. For completely unpolarized light, only S_0 remains. If the light is completely linearly polarized, S_3 is zero. Moreover, for completely polarized light, $S_0^2 = S_1^2 + S_2^2 + S_3^2$, otherwise $S_0^2 \geq S_1^2 + S_2^2 + S_3^2$.

Degree of linear polarization (DoLP), degree of circular polarization (DoCP) and degree of polarization (DoP) can be calculated by Stokes parameters as follows:

$$\mathrm{DoLP} = \frac{\sqrt{S_1^2 + S_2^2}}{S_0}; \mathrm{DoCP} = \frac{\sqrt{S_3^2}}{S_0}; \mathrm{DoP} = \sqrt{\mathrm{DoLP}^2 + \mathrm{DoCP}^2} \tag{2}$$

where DoLP, DoCP, and DoP are all between 0 and 1. For completely polarized light DoP = 1 and for unpolarized light DoP = 0.

Stokes parameters can be measured in different ways [27,29]. The measurement method used in this paper is to allow the input beam to propagate sequentially through two polarizing elements, namely, a quarter wave plate (QWP) and a linear polarizer (LP). The Stokes parameters are measured by first removing the QWP and then measuring the intensity of the outcoming optical beam with the transmittance axis of the LP set at an angle θ = 0°, 90°, 45° and 135° with respect to the x-axis of the Cartesian coordinate system (intensities I_1, I_2, I_3 and I_4, respectively). The final measurement is made by adding the QWP into the optical train before the LP, with its fast axis lying on the x-axis of the reference system (intensity I_5). For the final measurement, the angle of the LP is set to θ = 45°.

Then the four Stokes parameters can be found as

$$\begin{aligned} S_0 &= I_1 + I_2 \\ S_1 &= I_1 - I_2 \\ S_2 &= I_3 - I_4 \\ S_3 &= 2I_5 - S_0 \end{aligned} \tag{3}$$

#165278 - $15.00 USD Received 23 Mar 2012; revised 25 May 2012; accepted 28 May 2012; published 25 Jun 2012

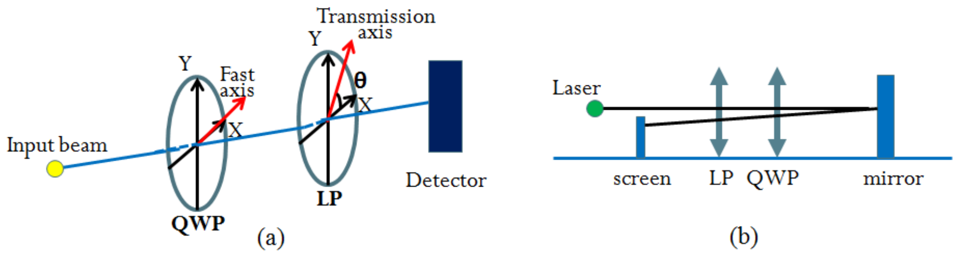

Fig. 1. (a) Measurement configuration of Stokes parameters. (b) Illustration of alignment experiment for LP and QWP.

Figure 1(a) shows the measurement configuration. Note that Eq. (3) holds only for ideal polarizing elements. Transmission efficiency of these elements has to be taken into account for a proper determination of the Stokes parameters with real polarizers and wave plates. However, an advantage of this measurement method is that we do not need to consider the transmission efficiency of the LP for the calculation of DoP, because it cancels out when using Eq. (2). Despite of this fact, the absorption factor of the QWP must be considered because both the LP and the QWP are inserted during the measurement of S_3.

As stated in [26], the accurate measurement of the Stokes parameters by this technique requires the precise alignment of the axis of both the LP and the QWP. In our experiments this adjustment is achieved by means of the setup shown in Fig. 1(b). In this experiment, a laser beam goes through the LP and the QWP and is reflected back onto a screen. We adjust the angle between the axis of the LP and the QWP until the intensity of the reflected dot reaches a minimum. A digital optical power meter can be utilized to measure the intensity. In this situation the angle between the transmission axis of LP and the fast axis of QWP is 45þ. This accurate alignment guarantees the correct measurement of S_3.

3. 3D polarimetric computational integral imaging system

In this section, we present a 3D polarimetric integral imaging system, including a polarimetric pickup process and a modified computation reconstruction process. By using this system, we can achieve a 3D polarimetric computational reconstruction under natural illumination conditions.

3.1 Pickup of polarimetric images

A typical pickup process in integral imaging is shown in Fig. 2(a). The direction and intensity information of the rays coming from 3D objects are recorded by a lenslet array or a sensor array [15]. The recorded images with their own perspective are referred to as elemental images. In this paper, we use a synthetic aperture integral imaging system (SAII) [30] which is performed by moving a digital camera on a two-axis translation stage. Compared to the conventional SAII, our polarimetric integral imaging uses two more optical components (LP and QWP) inserted in front of the image sensors to capture the polarimetric information of a 3D scene (Fig. 2(b)). In fact, the two optical components and the image sensor can be replaced by a single polarimetric image sensor, which can directly provide the measurement of Stokes parameters.

#165278 - $15.00 USD Received 23 Mar 2012; revised 25 May 2012; accepted 28 May 2012; published 25 Jun 2012

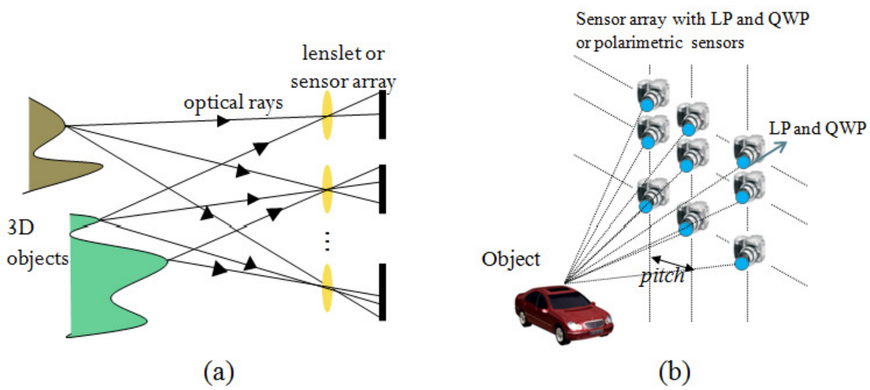

Fig. 2. (a) Pickup process of integral imaging. (b) Pickup process of polarimetric integral imaging.

3.2 Polarimetric information applied to computational image reconstruction

A computational 3D image reconstruction in integral imaging is described in [12] using the back projection technique. In this approach, each elemental image is projected back on the desired reconstruction plane. The reconstruction image plane consists of the average of all the back-projected pixels from the shifted elemental images. The collection of all the reconstruction image planes represents the volume reconstruction of a 3D scene.

In our proposed 3D polarimetric integral imaging system, the reconstruction images need to carry the 3D polarimetric information of objects. The conventional computational reconstruction method cannot implement the task directly since it does not consider polarimetric features of the scene. Therefore, we propose a modified computational reconstruction method based on a combination of the DoP and the original elemental images.

In our proposal, if we assume that the total number of elemental images is N, the image at the reconstruction plane, $R(x, y; z)$, at a distance z from the imaging system, is expressed as

$$R(x,y;z)=\begin{cases}\dfrac{1}{T}\displaystyle\sum_{k=1}^{N}\left(EI_k\left(x+\dfrac{c_x^k r^k}{M},\, y+\dfrac{c_y^k r^k}{M}\right)\right)*I\left(A_{DoP}^k\left(x+\dfrac{c_x^k r^k}{M},\, y+\dfrac{c_y^k r^k}{M}\right)>p\right) & \text{when } T\geq N_t\\ 0\quad (black) & \text{otherwise}\end{cases}\tag{4a}$$

$$T=\sum_{k=1}^{N} I\left(A_{DoP}^k\left(x+\frac{c_x^k r^k}{M},\, y+\frac{c_y^k r^k}{M}\right)>p\right)\tag{4b}$$

where EI_k represents the k-th elemental image, M is the magnification factor ($M = z/g$, g being the distance between the pickup plane and the image plane), r^k describes the number of pixels per unit distance for the k-th sensor, $\left(c_x^k, c_y^k\right)$ is the position of the k-th sensor, $A_{DoP}^k(x, y)$ represents the k-th DoP image, $I(\cdot)$ is an indicator function, p is a given threshold of degree of polarization ($0 \leq p \leq 1$), and N_t is a given number ($0 < N_t < N$).

The reconstruction technique stated in Eq. (4) is based on the following procedure: instead of using all the pixels from the shifted elemental images as the case in conventional back projection techniques, only the pixels whose DoP is greater than p are used to perform the 3D image reconstruction. T is the total number of the pixels whose DoP are larger than the given threshold p. In this way, we can implement polarimetric image reconstruction in 3D space. The condition in Eq. (4a), $T > N_t$, is used to reduce reconstruction errors caused by some artificial DoP information. N_t can be set as $N/4$ or $N/5$ based on the particular situation.

4. Experimental results

Before implementing the proposed 3D polarimetric integral imaging system, we need to select a proper QWP according to the performance of the image sensor. The sensor used in our experiments belongs to the Canon® 5D series. According to the quantum efficiencies of the three channels of this camera (see files from http://astrosurf.com/buil/50d/test.htm), we decided to use the G channel and a QWP designed for 543 nm from Melles Griot®. The spectral band tolerance width of this QWP is around 80 nm which matches the efficiency width of the G channel of our sensor. Moreover, the transmittance of the selected QWP is larger than 99.75%. We can ignore the absorption of our QWP when using Eq. (2) to calculate DoP information.

In the experiment, two plastic cars and some plastic trees are used as a 3D scene illuminated by natural light sources. These two plastic cars have more specular surfaces, like the doors and the windows, in comparison with the trees. Two cars (objects) are located approximately 530 mm away from the sensor array with a tree in front of them (occlusion) and some others behind them (background) at 450 mm and 720 mm from the sensors, respectively. Elemental images are captured with the proposed polarimetric integral imaging system, by moving a digital camera, assembled with the LP and the QWP in front of its lens, on a two-axis translation stage. Figure 3 shows the experimental setup. The focal length of the image sensor is 50 mm and the sensor size is 36 mm (W) × 24 mm (H) with square pixel shape. The pitch of the scan movement is 5 mm. The image size of the elemental images is 1248 (W) × 832 (H) and the total number of elemental images is 6 by 6.

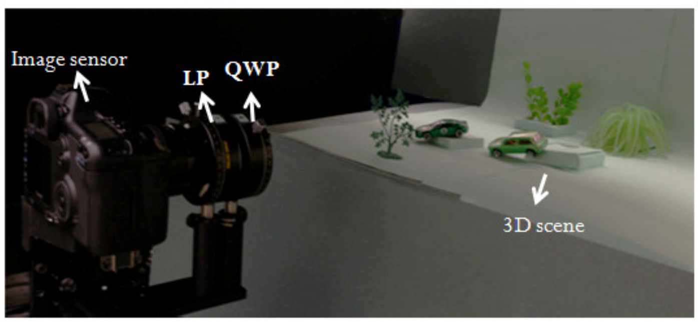

Fig. 3. Experimental setup of a polarimetric integral imaging system.

Four examples of elemental images are shown in Fig. 4. We selected *green* objects to compose the scene because we use the G channel of the image sensor. DoLP, DoCP and DoP images of the corresponding images in Fig. 4 are shown in Fig. 5 with the given color mapping. It can easily be seen that light coming from most of the surfaces of the cars is highly polarized in contrast to the ones of the occlusion and the background. Moreover, most of the polarization generated after reflection of the natural light is linear. From Fig. 5, we can also see a relatively high value of the polarization degrees around the edges of the occlusion, objects and background. In fact, these values are likely artifacts since the calculation of DoP for the image edges may have some errors because the images captured to measure Stokes parameters may have small shift bias when we rotate the LP to different angles (see Eq. (3)). If the shift distances among the images are large (more than 2 or 3 pixels), some methods should be used to obtain the corresponding shifted pixels and correct the images in order to reduce the measurement errors. In our experiment, we calculated the shift distances by using local correlation, which are approximately 1 pixel.

The 3D image reconstruction results from both conventional integral imaging and the proposed polarimetric integral imaging are illustrated in Fig. 6. Three different reconstruction planes located at 450 mm (occlusion), 530 mm (cars), and 720 mm (background) are shown. Figure 6(a) gives the reconstruction images by using the conventional reconstruction method, where the occlusion, the cars, and the background are focused. In Fig. 6(b)-6(c), the

#165278 - $15.00 USD Received 23 Mar 2012; revised 25 May 2012; accepted 28 May 2012; published 25 Jun 2012

reconstruction results by using the proposed polarimetric reconstruction method in Eq. (4) are presented. The threshold p for the DoP is set to 0.2 and 0.4, and N_t is fixed to $N/5$. In Fig. 6(b)-6(c), only the cars show up but the occlusion and the background do not appear on the

Fig. 4. Four examples of elemental images in our experiment

reconstruction images. This occurs because in our polarimetric integral imaging system only the objects emitting light with DoP larger than p are reconstructed in 3D space. Experimental results also show that occlusion can be mitigated in 3D image reconstruction when occlusion has a diffuse surface compared to the objects of interest. Moreover, the 3D reconstruction method may benefit the tasks of specific object detection or classification. However, in practical applications, the direction of the light source may need to be considered as the DoP images may vary with the orientation of illumination.

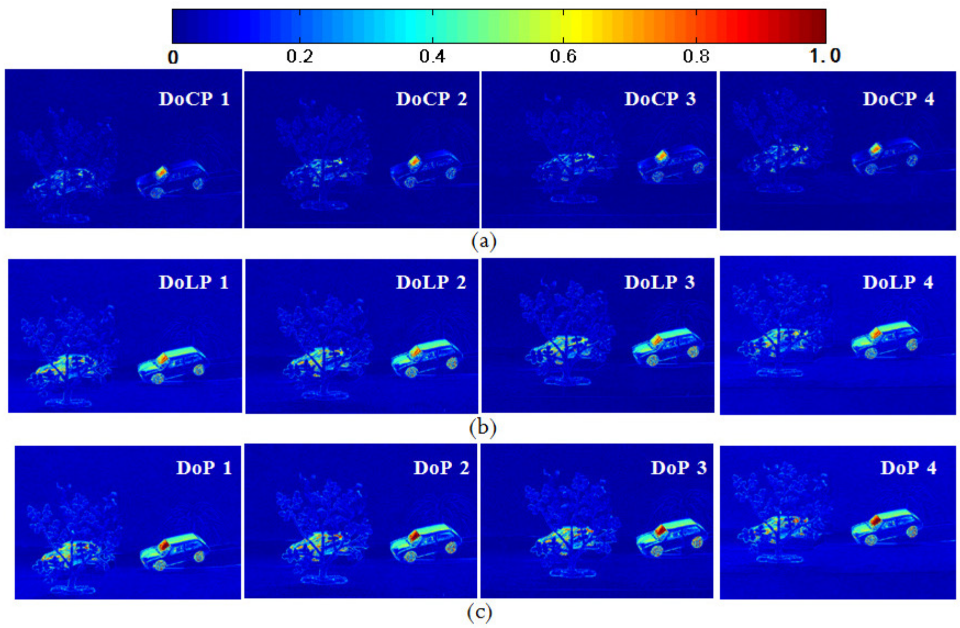

Fig. 5. DoLP, DoCP, DoP images of elemental images shown in Fig. 4. (a) DoLP images. (b) DoCP images. (c) DoP images.

5. Conclusion

In this paper, we have presented a 3D polarimetric integral imaging system based on distinct polarization characteristics of different object surfaces. The system can achieve 3D polarimetric image reconstruction by a modified computational reconstruction method. This technique is simply based on DoP images calculated from the measured Stokes parameters along each elemental image of the integral image. By performing the proposed system, only objects with specific polarization properties are reconstructed in 3D space. Experimental results are presented to verify the feasibility of the proposed system. The system may be used

#165278 - $15.00 USD Received 23 Mar 2012; revised 25 May 2012; accepted 28 May 2012; published 25 Jun 2012

to detect or classify objects with distinct polarization signatures in 3D space, and can support enhanced 3D imaging of polarized objects through diffuse occlusions.

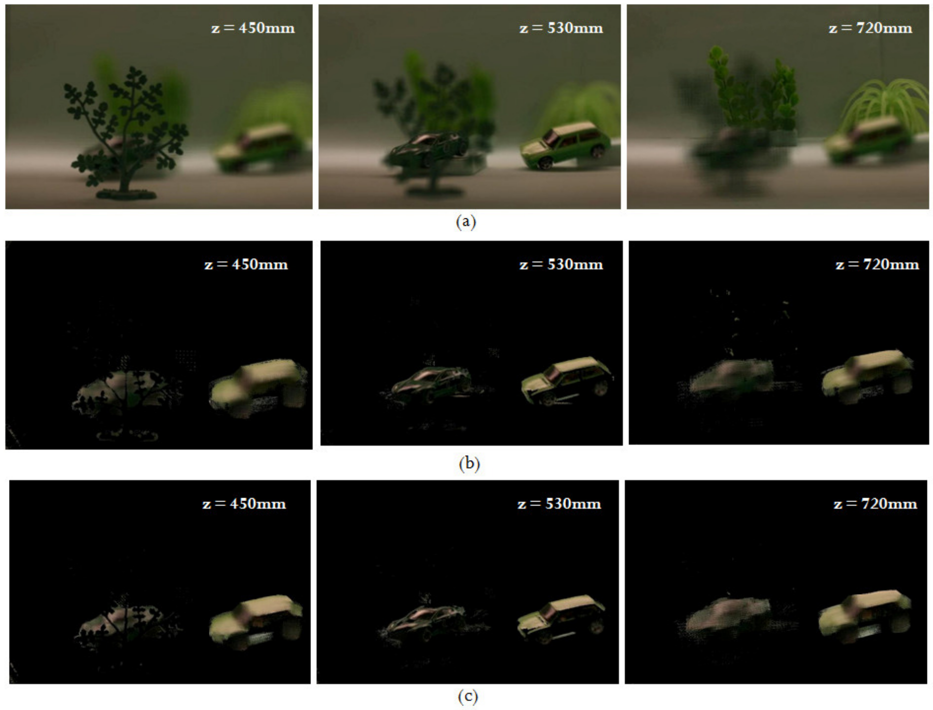

Fig. 6. Reconstruction results at 450mm, 530mm, and 720mm. (a) Reconstruction results of conventional integral imaging. (b) Reconstruction results of the proposed polarimetric integral imaging with $p = 0.2$. (c) Reconstruction results of the proposed polarimetric integral imaging with $p = 0.4$.

Acknowledgments

This work was supported in part by Defense Advanced Research Projects Agency (DARPA) and Air Force Research Laboratory (AFRL) under contract number FA8650-07-C-7740. The opinions presented in this paper do not and are not mean to represent the opinions of DARPA and AFRL. G. Saavedra and M. Martinez-Corral acknowledge the financial support of the Plan Nacional I + D + I under Grant FIS2009-9135, Ministerio de Ciencia e Innovación, Spain, and the Generalitat Valenciana under Grant PROMETEO2009-077.

#165278 - $15.00 USD Received 23 Mar 2012; revised 25 May 2012; accepted 28 May 2012; published 25 Jun 2012